

EXPERIMENTAL AND NUMERICAL STUDY OF DRYING-INDUCED WARPING OF CONCRETE SLABS

A.M. Alvaredo, S. Gallo, and F.H. Wittmann,
Laboratory for Building Materials,
Swiss Federal Institute of Technology Zurich

Abstract

A numerical model including a nonlinear diffusion analysis and the consideration of cracking is applied to the prediction of drying-induced warping of concrete slabs. Numerical results are compared with experimental values obtained for two mortar qualities. For most practical applications, the numerical predictions can be considered to be sufficiently accurate. Although these preliminary results show that more research is needed, some important practical conclusions can be drawn at this stage. One of them is that a more prolonged curing period does not prevent warping. Further, mixes aimed at creating an open pore structure appear to reduce warping significantly.

1 Introduction

An approach towards the consideration of the stresses induced by temperature or moisture changes in concrete members has been described in detail in Alvaredo (1994) and outlined in another contribution to this volume (Alvaredo, 1995). The numerical model has

been developed and validated by comparison with shrinkage tests (Alvaredo, 1994) in order to be applied to the solution of relevant practical problems. One of them is, undoubtedly, the warping of concrete slabs exposed to asymmetric drying. By means of an extensive parametric study, it has been shown in Alvaredo and Wittmann (1995a, 1995b) that, contrary to some wide-spread beliefs in practice, warping can neither be controlled by increasing the depth of the slabs, nor by increasing the tensile strength or the period of curing, nor by reducing the distance between joints within a practical range. Some of these design variables only exert an influence on the time at which the maximum warping occurs; others merely activate the competition between opposing mechanisms. As for the effect of fibres, the results of the numerical study indicate that the maximum warping attained by slabs of fibre reinforced concrete, or the restraint reaction necessary to prevent warping by means of dowels, is slightly higher than for normal concrete. The main advantage of the addition of fibres lies in the resulting crack pattern: the increased fracture energy reduces the severity of cracking. Further results demonstrate that the application of a coating acting as vapour barrier can be used as an efficient technological means for the control of warping.

Although the outcome of the parametric study seemed reasonable and promising, an important question still remained unanswered: does the numerical model capture the essentials of the phenomena involved in drying-induced warping? Since only the comparison between numerical predictions and experiments can provide the degree of accuracy of a numerical model and point at the necessary improvements, we decided to carry out warping tests. The main results as well as the agreement with the numerical predictions will be discussed in the next sections. It should be mentioned here that results of similar tests have been published recently (Peteln, 1995).

2 The numerical model and required material parameters

The numerical model consists, first, of a nonlinear diffusion analysis for the calculation of the time-dependent distribution of relative humidity and, second, of a subsequent stress analysis including cracking and the consideration of the nonlinear boundary conditions due to lack of contact between the warping slab and the subgrade.

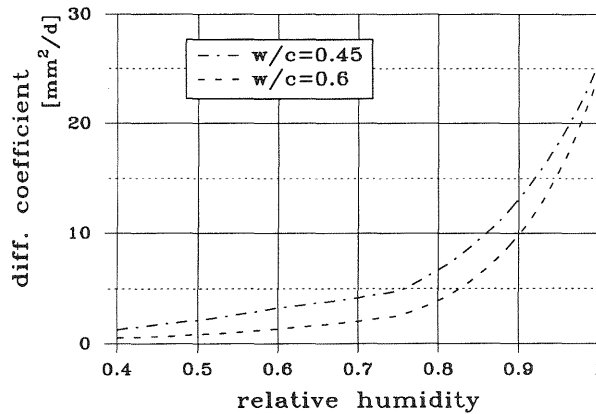


Figure 1: Relationship between relative humidity and diffusion coefficient obtained for two mortar qualities

Its highlights have been described in another contribution to this volume (Alvaredo, 1995); the thorough discussion and justification of each of the underlying assumptions can be found in Alvaredo (1994). A case with different mechanical boundary conditions, the behaviour of a thick coating bonded to a concrete slab, is dealt with in a separate contribution to this volume (Martinola and Wittmann, 1995).

The relationship between the moisture diffusion coefficient D and the relative humidity h was obtained by means of inverse analysis of drying tests, as described in Section 3.2 in Alvaredo (1995). The curves corresponding to the two mortar mixes characterized in the next section are shown in Fig. 1. It might seem surprising that the diffusion coefficient of the mortar with the lower water/cement ratio, $w/c = 0.45$, is higher than the diffusion coefficient of the mortar with $w/c = 0.6$. The explanation for this lies in the open pore structure of the former mortar quality, which, as will be mentioned in the next section, is typical of mixes used in practice for floating overlays. The presence of macropores enhances moisture transport and thus results in a higher moisture diffusion coefficient.

The determination of the coefficient of shrinkage, α_{sh} , by means of inverse finite element analysis of shrinkage tests at three different air relative humidities has been described in Section 3.2 in Alvaredo (1995). The obtained $\alpha_{sh} - h$ relationship for the two mortar qualities considered in this experimental work is illustrated in Fig. 4 in that reference.

As will be described in the next section, the tested concrete plates

were moist cured. For this reason, drying shrinkage for relative humidities close to saturation cannot be expected to reach its maximum, as was the case for the shrinkage of the water cured cylinders used to fit the $\alpha_{sh} - h$ relationship. Hygral calculations were therefore carried out by assuming an initial relative humidity $h_o = 0.95$. With respect to the boundary conditions, the specimens were considered to be exposed to air at $h_a = 0.4$ at their top side only; along this surface, a value of the film coefficient $H_F = 5$ mm/day was used in the analysis. Moisture flux through the remaining sides was prevented.

The dead weight was taken into consideration in the analysis by applying to all elements in the finite element discretization a downward volume load equal to the measured apparent densities, 2.29 kg/dm³ for the mortar with $w/c = 0.45$ and 2.285 kg/dm³ for the mortar with $w/c = 0.6$.

The fracture mechanics parameters required for the analysis of crack formation were obtained by inverse analysis of the load-displacement curves recorded during wedge splitting tests (Brühwiler and Wittmann, 1990). The following values were found to characterize both mortar qualities: for $w/c = 0.45$, $\bar{E} = 35000$ MPa, $\bar{f}_t = 3.3$ MPa, $\bar{G}_F = 125$ N/m and a break-point of the bilinear strain softening diagram at a stress of 1 MPa and an opening displacement of $3.02 \cdot 10^{-2}$ mm.; for $w/c = 0.6$, $\bar{E} = 28000$ MPa, $\bar{f}_t = 3.3$ MPa, $\bar{G}_F = 82$ N/m and a break-point of the bilinear strain softening diagram at a stress of 0.75 MPa and an opening displacement of $1.56 \cdot 10^{-2}$ mm. The respective softening diagrams are indicated in Fig. 2. It is worth pointing out that the relatively low value of \bar{f}_t and the relatively high value of \bar{G}_F for the mix with $w/c = 0.45$ can be linked with its open pore structure.

As described in Alvaredo (1994), gap-friction elements were introduced at the nodes on the bottom side of the finite element discretization with the aim to represent, on the one hand, the stiffness of the foundation and, on the other, the lack of contact induced by warping. The results presented in Section 4 were obtained by assuming an almost infinitely stiff subbase-subgrade system (see Alvaredo and Wittmann, 1995b).

Calculations were carried out under the assumption of plane stress and symmetry conditions, i.e. for a finite element discretization of depth d , length $l/2$ and thickness b , as indicated in Fig. 3.

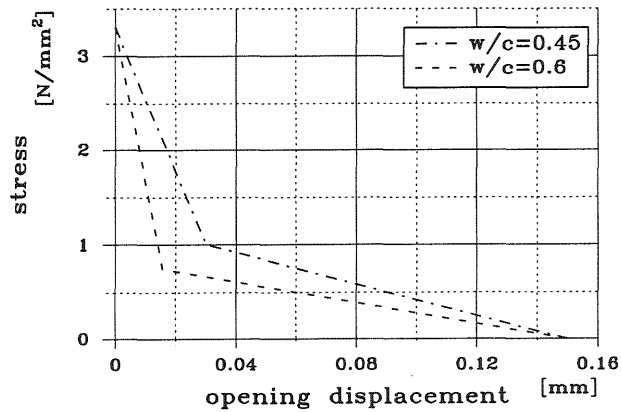


Figure 2: Bilinear strain softening diagrams of mortar qualities used in experiments

3 Experiments

Two mortar qualities were tested. One of them, with $w/c = 0.45$ and characterized by an open pore structure, can be considered to be representative of mixes used in practice for floating overlays. For comparison, a second quality, deliberately composed so as to exhibit higher shrinkage, was included in the study. Both of them had a maximum size of aggregate of 8 mm. The mix with $w/c = 0.45$ had 350 kg of Portland cement per cubic metre, whereas the cement content of the mix with $w/c = 0.6$ was 400 kg/m³. For the first mix, workability was enhanced by adding 1.5% of superplasticizer (referred to the weight of cement).

Three experimental series were carried out. For the first of them, consisting of two specimens of each mix, the lateral sides of the prismatic concrete plates were coated with epoxy resin to avoid moisture loss. After demoulding, the specimens were laid on a polyethylene sheet in order to reduce friction with the floor. For the second and third series, consisting of one specimen of each mix, the lateral and bottom sides were covered with a polyethylene sheet fixed to the specimens by means of tapes. This was done with the aim to prevent moisture loss through the bottom surface, which would have otherwise started as soon as warping reached an a priori unknown value (this happened during the first experimental series).

In all cases, the top side of the plates was exposed to the unconditioned laboratory air. For the first series, h_a varied between 48% and 54% without a systematic tendency. The plates of the second

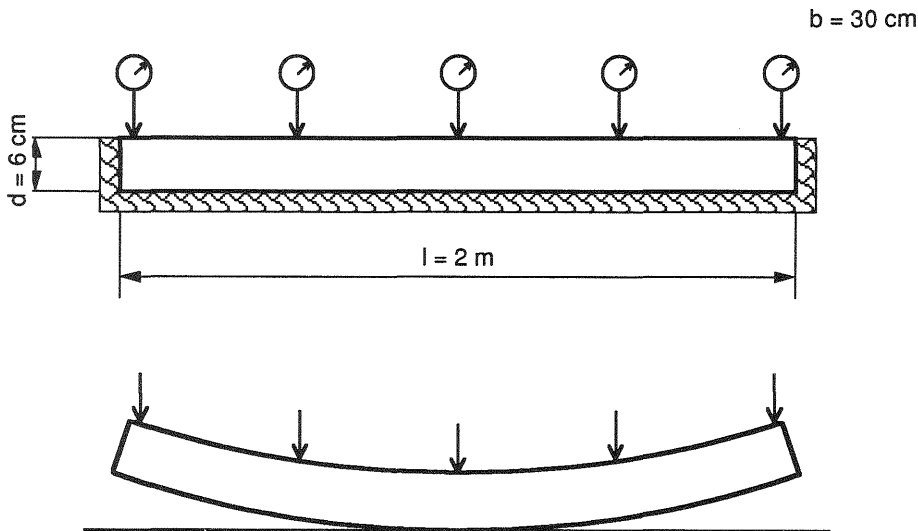


Figure 3: Schematic representation of the specimens geometry and the experimental set-up

series were exposed to $\bar{h}_a = 0.41$ for the first 10 days of drying and to $\bar{h}_a = 0.33$ further on. For the last series, $\bar{h}_a = 0.44$ was the average value of air relative humidity for $t \leq 46$ days and $\bar{h}_a = 0.54$ thereafter. These strong oscillations are associated with seasonal variations.

The specimens, whose geometry is illustrated in Fig. 3, were kept under wet burlap until the beginning of the measurements. For the first and second series, drying at the top surface started at an age of 5 days; for the last series, the age was 28 days. Once drying started, warping was recorded as function of time by means of inductive displacement transducers, equidistantly spaced by 489 mm, placed at the locations schematically indicated in Fig. 3. Further details of the experiments are described in an internal report (Gallo, 1994).

4 Results

Because of material heterogeneities, imperfections in the manufacture of the specimens, etc., it cannot be expected that the drying specimens deform entirely symmetrically. The experimental warping was thus defined as the relative vertical displacement between the centre of the plate and the average value of the indications of the first and last transducers in Fig. 3. The numerically predicted

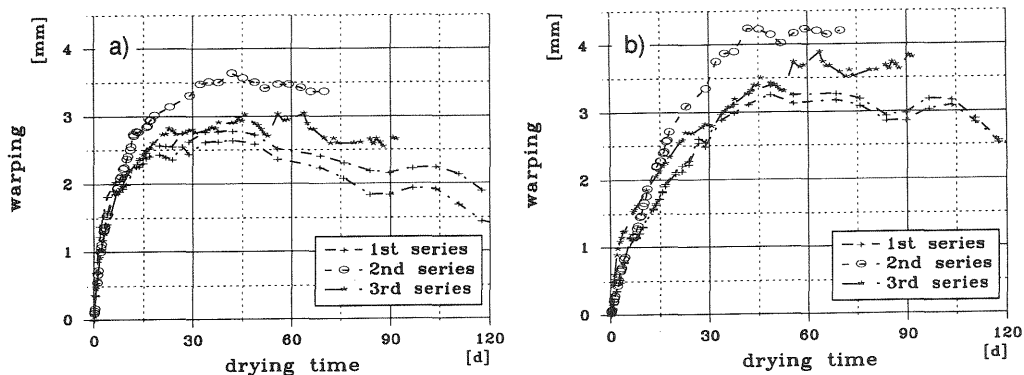


Figure 4: Evolution of warping with drying time for concrete plates of three experimental series: a) for $w/c = 0.45$; b) for $w/c = 0.6$

warping was obtained as the relative vertical displacement between the edge and the centre measured along the top surface of the finite element discretization.

Figs. 4a and 4b show the evolution of warping with drying time as determined experimentally for both mortar mixes. Two comments can be made in reference to these figures. First of all, warping of the specimens of the first series is lower than for the second series, although drying started at the same age. The explanation for this is two-fold: the average air relative humidity was lower during the tests of the second series and, in addition, some moisture loss through the bottom surface probably reduced the magnitude of the differential shrinkage of the specimens of the first series. The second interesting observation is that the evolution of warping with drying time for the specimens of the third series, tested at the age of 28 days, is nearly the same as the observed behaviour of the other two series. It might be even speculated that, had the air relative humidity for the second and third series been the same, the maximum warping for the third series would have been at least the same as for the second series, tested at the age of 5 days. A conclusion of great practical importance can be drawn: a more prolonged period of curing does not at all prevent drying-induced shrinkage. For the reasons discussed in Section 4.1 in Alvarado (1995), the general tendency is that shrinkage, and with it warping, increases with the age at exposure to drying.

The evolution of warping predicted for both water/cement ratios is compared with the experimental results of the second and

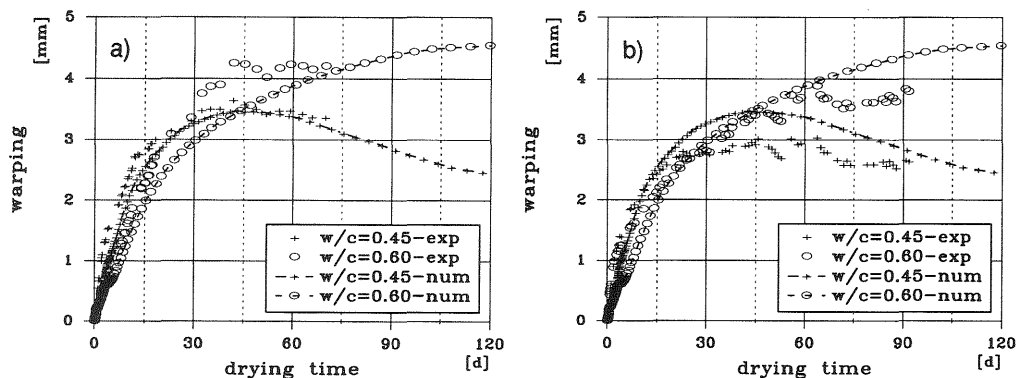


Figure 5: Comparison between numerical evolution of warping and experimental results: a) for the second series; b) for the third series

third series in Figs. 5a and 5b, respectively. As was mentioned in Section 2, the numerical curves were obtained for $h_a = 0.4$. However, the average air relative humidity for the second experimental series was, in general, lower and for the third series higher than the value used in the calculations (see Section 3). This explains why the numerical curves lie below the experimental ones in Fig. 5a and above them in Fig. 5b. It is interesting to note that both the experimental and the numerical development of warping for the mix with $w/c = 0.6$ are slower than for the other mortar quality, due to the lower diffusion coefficient of the mix with $w/c = 0.6$. The lower modulus of elasticity, E , and the higher coefficient of shrinkage, α_{sh} , of the richer mix are among the reasons why it attains a higher maximum warping. It can be said that, in general, the numerical prediction agrees better with the experimental behaviour of the mix with $w/c = 0.45$ than with that of the mix with $w/c = 0.6$.

The distribution of vertical displacements along the top side of the finite element discretization at about 50 days of drying is compared with the corresponding experimental values corresponding to the second and third series for the mortar mixes with $w/c = 0.45$ and $w/c = 0.6$ in Figs. 6a and 6b, respectively. Both the numerical and the experimental results have been referred to the vertical displacement of the centre of the specimens.

With the aim to contribute to the discussion on the accuracy of the numerical predictions, the four experimental curves determined for the mortar mix with $w/c = 0.6$, for which the agreement between experiments and numerical predictions is less good, are

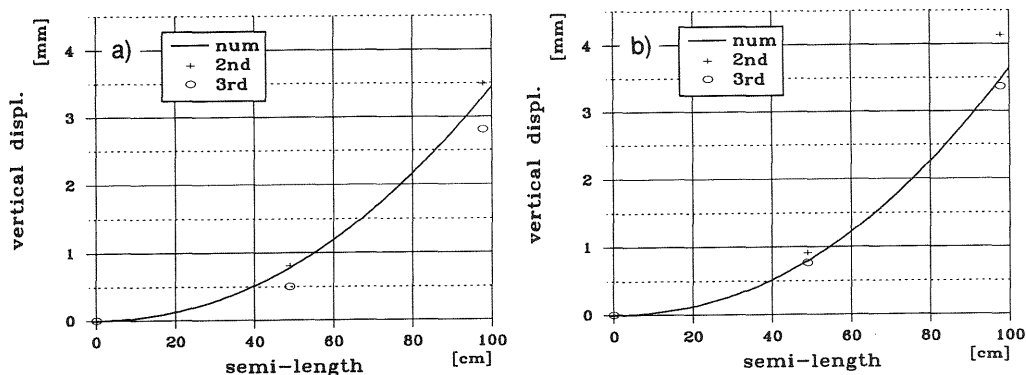


Figure 6: Distribution of vertical displacements referred to the centre of the specimens at about 50 days of drying: a) for $w/c = 0.45$; b) for $w/c = 0.6$

compared with two numerical curves in Fig. 7. The one referred to as “e.s.”, calculated under the assumption of an elastic-softening material behaviour, coincides with the numerically predicted evolution of warping for this mix shown in Figs. 5a and 5b. The other curve, referred to as “l.e.”, corresponds to a linear elastic stress analysis. By comparing both numerical curves it is evident that the extensive formation of fracture process zones in this relatively brittle material (see strain softening behaviour in Fig. 2) reduces warping significantly. However, the general tendency of the time-dependent warping observed experimentally is not fully captured by the numerical analysis including the consideration of cracking either.

5 Discussion and conclusions

It can be said that, for most practical applications, the numerical predictions are sufficiently accurate (see Figs. 5a, 5b, 6a and 6b). Fig. 7 proves that a linear stress analysis is inappropriate and that the consideration of cracking drastically improves the agreement with experimental results. However, it is evident that not all the relevant parameters involved in time-dependent warping are described precisely by the numerical model presented here. This is especially true for the mix with $w/c = 0.6$.

Further research, both experimental and numerical, is needed. Possible topics are the influence of creep and of sustained load on the formation and propagation of fracture process zones and cracks.

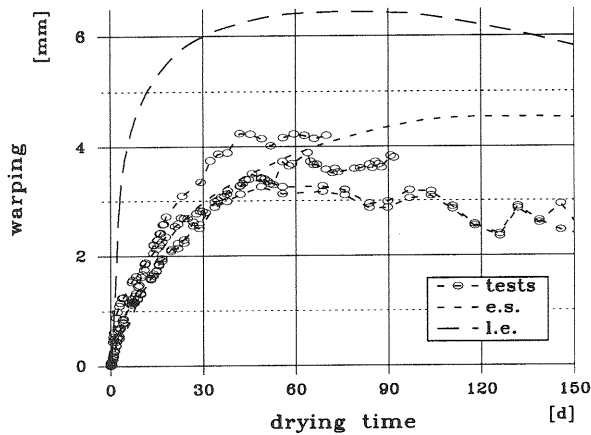


Figure 7: Experimental response of the mix with $w/c = 0.6$ compared with two numerical predictions

Yet, some conclusions of practical consequences can be drawn at this stage. One of them is concerned with the influence of the curing period. It has been shown that a more prolonged curing does not prevent warping. Moreover, it has been observed experimentally and predicted by means of the numerical model that mixes characterized by an open pore structure produce less warping. The method described in this contribution can also be applied to optimize mix proportions with respect to warping.

References

- Alvaredo, A.M. (1994) Drying shrinkage and crack formation. **Building Materials Reports**, 5, Aedificatio, Freiburg, Germany.
- Alvaredo, A.M. (1995) Crack formation under hygral or thermal gradients, in this volume.
- Alvaredo, A.M. and Wittmann, F.H. (1995a) Influence of material properties on cracking and warping of a drying concrete ground floor, in **Industrial Floors '95** (ed P. Seidler), Techn. Akademie Esslingen, Esslingen, Germany, 201-207.
- Alvaredo, A.M. and Wittmann, F.H. (1995b) Influence of geometry and boundary conditions on cracking and warping of a drying concrete ground floor, in **Industrial Floors '95** (ed P. Seidler), Techn. Akademie Esslingen, Esslingen, Germany, 209-218.
- Brühwiler, E. and Wittmann, F.H. (1990) The wedge splitting test, a new method of performing stable fracture mechanics tests. **Engng. Fract. Mech.**, 35, 117-125.

-
- Gallo, S. (1994) Untersuchung der Eigenschaften von Kunststoffaserbeton hinsichtlich seiner Verwendung für schwimmende Unterlagsböden. Semesterarbeit WS 1993/1994, Lab. for Building Materials, Swiss Federal Institute of Technology Zurich.
- Martinola, G. and Wittmann, F.H. (1995) Optimization of mortars by means of fracture mechanics, in this volume.
- Peteln, A. (1995) Verringerung des Aufschüsselns, in **Industrial Floors '95** (ed P. Seidler), Techn. Akademie Esslingen, Esslingen, Germany, in the supplement.

